JOURNAL OF SOLID STATE CHEMISTRY 43, 87–96 (1982)

Spectroscopic Properties of $Ln_2MoO_6:Eu^{3+}$

JINGGEN HUANG* AND JEAN LORIERS

Laboratoire d'Etude des Matériaux par Techniques Avancées, E.R. 211 du CNRS, 1 place A. Briand, 92190 Meudon-Bellevue, France

AND PIERRE PORCHER

Laboratoire des Eléments de Transition dans les Solides, E.R. 210 du CNRS, 1 place A. Briand, 92190 Meudon-Bellevue, France

Received December 9, 1981; in final form February 16, 1982

The spectroscopic properties of $Ln_2MoO_6:Eu^{3+}$ (Ln = La, Gd, Y) compounds were investigated. The differences in the recorded fluorescence spectra are in accord with the different structures. For the $La_2MoO_6:Eu^{3+}$ case, the spectrum is compatible with a C_2 point site symmetry. It appears that the energy level scheme is connected with the rare earth oxychloride one, so it is possible to determine accurately sets of crystal field parameters simulating the spectrum. For the other compounds, the Eu^{3+} ions occupy three different point sites. By using the site-selective excitation on the $^5D_0$ level it is possible to identify the energy level scheme characterizing each point site.

Introduction

The Ln_2O_3–Mo_2O_3 chemical system (Ln = rare earth + Y) constitutes a very rich family of compounds having different stoichiometric formulas and different structures. For instance, it is possible to synthesize compounds where the rare earth/molybdenium oxide ratio can be equal to $\frac{3}{1}$, $\frac{2}{1}$, $\frac{1}{1}$, $\frac{1}{3}$, $\frac{1}{4}$, etc. (*1–9*). Some of these compounds have interesting physical properties (*7, 9–11*). But because of the number, the type, and the varieties of point site symmetries occupied by the rare earth ion, this series did not receive considerable attention from a spectroscopic point of view (*12–14*). This paper constitutes the first article of a series where the spectroscopic properties of the europium ion, embedded in these materials, will be studied in terms of local structural probe analysis and, when possible, in terms of parametrization of the crystal field effect.

Crystallographic Background

The rare earth oxymolybdates (1 : 1) do not constitute an isostructural series. Different structures exist depending on both the rare earth atom and on the synthesis conditions. The structure of La_2MoO_6 was determined by Sillen as early as 1943 (*3*). The system is tetragonal, a = 4.089, c = 15.99 Å, with $I\bar{4}2m$ as space group. The structure can be described in terms of $(LnO)_n^{n+}$ complex cation layers, showing analogy with the rare earth oxychloride

* Permanent address: Department of Chemistry, Fudan University, Shangai, China.

0022-4596/82/070087-10$02.00/0

(*15, 16*) and with a great number of oxysalts (*15, 17*). As a consequence the formula might be written as $(LaO)_2 MoO_4$. The lanthanum is coordinated to six oxygens. Four of them constitute a square plane creating the La_2O_2 group with a La–O distance of 2.38 Å. The two remaining oxygen atoms have a lower La–O distance, 2.33 Å. Thus the symmetry of the point site occupied by the rare earth is C_{2v}. For the other compounds of the series the usual phase has a completely different structure. It has been resolved for Sm_2MoO_6 (*19*), which is isomorphous to the gadolinium and the yttrium compounds. It can be described in the monoclinic system (*17, 19*) with *C2/c* as space group, derived from the scheelite structure. In this case, the rare earth atoms are coordinated to eight oxygens and occupy three different crystallographic positions, two 4*e* (with C_2 as point site) and one 8*f* (with C_1 as point site).

Preparation of the Compounds

All the samples here studied were prepared by using high-purity oxides as starting materials. The rare earth oxides were prefired at 800°C for some hours for dehydration and decarbonization. The synthesis method consists in a firing of the intimate rare earth and molybdenium oxide mixture, in the right proportions. The optimal heating conditions are a preheating of the mixture at 500°C for 12 hr, then a firing at 1000°C for 20 hr. All compounds were routinely checked by X-ray powder analysis, and appeared to be free of other phases.

Spectroscopic Measurements

These measurements were performed at 77 and 300K on samples doped by 2% of europium for La_2MoO_6 and 5% for Gd_2MoO_6 and Y_2MoO_6. Excitation spectra were recorded by using a double-beam Cary 17 spectrometer. The classical fluorescence spectra were obtained by using long uv lines of an OSRAM mercury lamp, selected by a wide-band Wood filter. The analysis of the fluorescence light was performed through a 1-m Jarrel Ash monochromator by using standard techniques. Because of a relatively high $^5D_0 \rightarrow {}^7F_0$ transition probability it was possible to selectively excite the $^5D_0$ level. For this, we used a Spectra Physics tunable dye laser equipped with Rhodamine 6 G as dye. As a consequence of the relatively low energy transfer from site to site, it was not necessary to use the time-resolved spectroscopy for the multisite compound analysis.

Analysis of the Spectra

Although the rare earth oxymolybdate series does not constitute an isostructural series, some common features have to be underlined. For instance, the excitation spectra are not very different for the three compounds. As a consequence of the low luminosity of the apparatus used, only the position of the charge transfer state (CTS) from O^{2-} to Eu^{3+} was recorded. For the three compounds, the maxima of the band are located at about 32,500, 28,300, and 28,200 cm^{-1} for La_2MoO_6, Gd_2MoO_6, and Y_2MoO_6, respectively. In the same way,

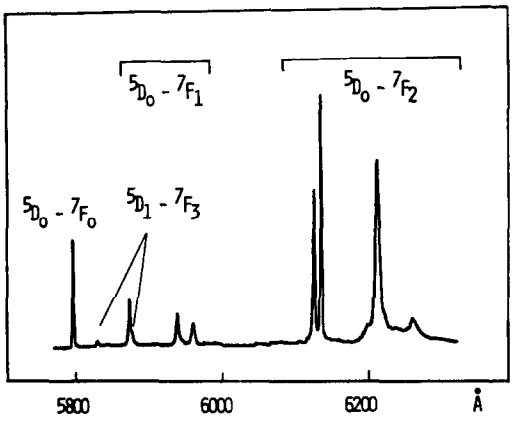

FIG. 1. The characteristic fluorescence spectrum of $La_2MoO_6:Eu^{3+}$ at 77K.

TABLE I

THE ENERGY OF THE OBSERVED TRANSITIONS IN THE FLUORESCENCE SPECTRUM OF La_2MoO_6: Eu^{3+} at 77K

Transition	I_{rel}	(Å)	E (cm^{-1})	Transition	I_{rel}	(Å)	E (cm^{-1})
$^5D_1$–$^7F_0$	15	5,256	19,026	$^5D_1$–$^7F_3$	10	5,866	17,047
	15	5,260	19,012	$^5D_0$–$^7F_1$	100	5,875.5	17,020
	100	5,274	18,961	$^5D_1$–$^7F_3$	20	5,880	17,006
					15	5,894	16,966
$^5D_1$–$^7F_1$	10	5,318.5	18,802		10	5,897.5	16,956
	10	5,322	18.790		5	5,901.5	16,945
	100	5,337	18.737		10	5,905.5	16,933
	5	5,374	18.607		5	5,916	16.903
	15	5,389	18.556		5	5,922.5	16.885
	15	5,407	18.495				
				$^5D_0$–$^7F_1$	80	5,939	16.838
					70	5,960	16.778
$^5D_1$–$^7F_2$	75	5,525	18.099				
	25	5,528.5	18.088	$^5D_0$–$^7F_2$	35	6,126.5	16,322
	10	5,532.5	18.075		45	6,136.5	16,296
	50	5,536.5	18.062				
	100	5,544	18.038		100	6,211	16,100
	80	5,552.5	18.018		10	6,258.5	15,978
	5	5,593	17.879				
	5	5,597	17,866	$^5D_0$–$^7F_3$	40	6,479	15,434
	10	5,613	17,816		75	6507.5	15,367
					90	6,521.5	15,334
$^5D_0$–$^7F_0$	100	5,798.5	17,246		75	6,541	15,288
					100	6,549.5	15,268
$^5D_1$–$^7F_3$	100	5,832	17,147		5	6,582	15,192
	25	5,837	17,133				
	10	5,844	17,112	$^5D_0$–$^7F_4$	10	6,957	14,374
	5	5,848	17,100		5	6,967.5	14,352
	15	5,845.5	17.081		1	7,023.5	14,238
	5	5,860	17,065		100	7,053	14,178
	10	5,864	17,053			7,056	14,172

the fluorescence spectra are mainly constituted by emissions from the $^5D_0$ level. At room temperature, no emission lines from other levels were recorded, showing a complete quenching of the upper levels. But, at 77K it was possible to observe well-resolved transitions from $^5D_1$, having a reasonable intensity, whereas emission from $^5D_2$ and $^5D_3$ were not observed.

A. La_2MoO_6:Eu^{3+}

At 77K the fluorescence spectrum of La_2MoO_6:Eu^{3+} is constituted by about 50 well-resolved lines (Figs. 1 and 2, Table I).

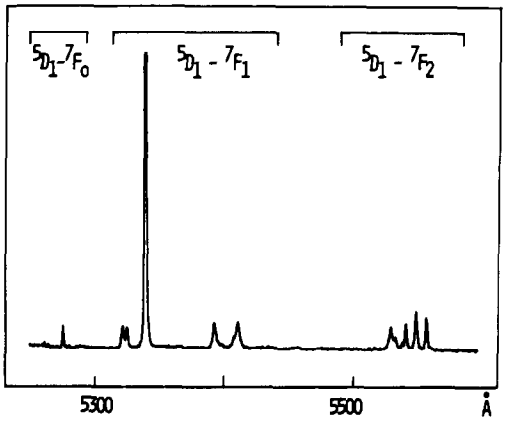

FIG. 2. Part of the fluorescence spectrum of La_2MoO_6:Eu^{3+} at 77 K.

The average linewidth is 10 cm^{-1}. The spectrum observed is rather simple, showing that the rare earth occupies only one point site. When the $^5D_0$ is selectively excited by the dye laser, only fluorescence from this level is observed. A comparison with the other transitions allows us to construct a partial energy level scheme of the ground ^7F multiplet for the Eu^{3+} ion.

By application of both group theory and electronic transition selection rules, it is possible from the spectrum to estimate the symmetry of the point site occupied by the rare earth. It is known (*20*) that the $^5D_0 \rightarrow {}^7F_0$ transition occurs only for C_s, C_n, and C_{nv} as point site symmetry. Moreover, the three lines observed for the $^5D_0 \rightarrow {}^7F_1$ magnetic dipole transition do not allow a symmetry higher than C_{2v}. But some ambiguities remain from the number of lines observed for the other transitions. Effectively we note, respectively, four, six, and five lines for the $^5D_0 \rightarrow {}^7F_2$, $^5D_0 \rightarrow {}^7F_3$, and $^5D_0 \rightarrow {}^7F_4$ transitions. A C_{2v} point group should allow four, five, and seven lines. When the number of observed lines is lower than the authorized number, one can suppose that the intensity parameters extinguish some of the transitions. But we note unambiguously six lines for $^5D_0 \rightarrow {}^7F_3$. Probably, it means that the real point site of the Eu^{3+} ion is slightly distorted from the ideal one proposed by Sillen (*3*). This observation has to be associated to ESR measurements (*21*) showing a lower symmetry of the site, and to the structure of the lanthanum oxysulfate, where the rare earth occupies a C_2 symmetry site, in an orthorhombic structure very close to the tetragonal structure of the lanthanum oxymolybdate. In order to explain this difference Kuvshinova *et al.* (*21*) argued that the spatial group of the lanthanum oxymolybdate should be I_{422} with C_2 as point group for the rare earth.

The whole appearance of the spectrum is analogous to that of other oxysalts: oxychlorides (*22*), oxysulfates (*23*), oxycarbonates (*24*). More precisely, the energy level scheme deduced from the spectrum is not far from the rare earth oxychloride one (*22*). For all these compounds the tetragonal $(LnO)_n^{n+}$ layer constitutes the framework of the structure. It was shown that this entity gives its "finger print" to the spectroscopic properties. The influence of this entity on the crystal field is more important than the other neighboring (*23*). Here too, the $^5D_0 \rightarrow {}^7F_0$ intensity is large. This transition is only allowed through the J-mixing effect (*25*). Its intensity mainly depends on the absolute value of B_0^2 (*26*).

B. Gd_2MoO_6:Eu^{3+} and Y_2MoO_6:Eu^{3+}

The fluorescence spectra of the Eu^{3+} ion in these materials are very different from the case of the lanthanum oxymolybdate. This is to be correlated with variations of the crystalline structure along the rare earth series. The spectra are rather complicated, but similar. For Gd_2MoO_6:Eu^{3+} we observe three distinct $^5D_0 \rightarrow {}^7F_0$ transitions located at 17,295, 17,282, and 17,212 cm^{-1}. This feature indicates at least three different point sites occupied by the rare earth. For Y_2MoO_6:Eu^{3+} only two $^5D_0 \rightarrow {}^7F_0$ transitions are observed, at 17,273 and 17,206

cm^{-1}, but from the complexity of the other wavelength ranges it can be assumed that either one of the three transitions is not allowed by the selection rules or, more probably, the $^5D_0 \rightarrow {}^7F_0$ lines are superimposed for two of the sites. The occurrence of three point sites is in accord with the structure of Sm_2MoO_6 (*19*) showing that the samarium atom occupies three different crystallographic positions (two 4*e* and one 8*f*).

From the classical uv excitation of the fluorescence, recorded at 77 K, it is not possible to recognize the origin of the transitions and to attribute one observed line to a particular site. Fortunately, the $^5D_0 \rightarrow {}^7F_0$ transitions are not only observed with a reasonable intensity in these compounds, but also some of them are well separated in energy. So, it is possible to selectively excite all $^5D_0$ levels by using a tunable dye laser.

Figure 3 shows the results obtained for such selective excitation in the case of $Gd_2MoO_6:Eu^{3+}$; the upper spectrum is the classical fluorescence spectrum given for comparison. For this compound a direct excitation of the sites called A and B does not completely extinguish fluorescent lines from the other sites A, B, or C. On the contrary, the direct excitation of site C, having the lowest $^5D_0$ energy, eliminates quite completely the emissions from the other sites. It is probably due to the low anti-Stokes transition probability from the $^5D_0$ (C) to the $^5D_0$ (A or B) level. For sites A and B, because of the great variability of the intensity of the fluorescent lines, under selective excitation wavelength, it is also possible to attribute each line to its site. Only a very few number of ambiguities remain when several lines are in accidental coincidence. From these experiments, it is possible to construct a partial energy level scheme for the ^7F_J ($J = 0$–4) levels (Table II).

On the other hand, the case of $Y_2MoO_6:Eu^{3+}$ is much more complicated (Fig. 4). We noted earlier that the $^5D_0$ levels corresponding to sites A and B are probably superimposed. Moreover, the third $^5D_0 \rightarrow {}^7F_0$ transition intensity is too weak to perform direct excitation. However, when the excitation wavelength is slightly changed about the $^5D_0$ energy position, the relative intensities of the lines corresponding to sites A and B change significantly, but not as drastically as for $Gd_2MoO_6:Eu^{3+}$, whereas the relative intensities corresponding to site C remain quite invariant. In order to confirm these attributions, some additional measurements through the $^7F_1 \rightarrow {}^5D_0$ transition were performed. The lowest $^7F_1$ Stark levels of sites A and B stand at 169 and 172 cm^{-1}, respectively. So, at 77 K, the remaining thermal population of these levels is about 5%, sufficient to initiate the $^7F_1 \rightarrow {}^5D_0$ transition, and to obtain significant results. For site C, the $^7F_1$ lowest Stark level is located at 293 cm^{-1}. Such a method is not applicable at 77 K, but measurements performed at 300 K (when the thermal population of this level is about 20%) confirm the assignment, in spite of the broadening of the lines due to the increase in the temperature. Finally, it is also possible to construct an energy level scheme for the three sites of $Y_2MoO_6:Eu^{3+}$ (Table II).

From the energy level schemes constructed for $Gd_2MoO_6:Eu^{3+}$ and $Y_2MoO_6:Eu^{3+}$, all the level degeneracies appear to be lifted. The application of both the group theory and electronic transition rules does not allow such a number of lines for a point symmetry higher than C_2. The number of crystal field parameters involved are 14 in this case. Moreover, there is no structural evidence showing that the point site symmetry can be considered as a distorted one from a high symmetry. Then it is not reasonable to simulate the experimental splitting of the level by using the crystal field theory. On the contrary, the same argument authorizes us to parametrize the crystal field effect on the lanthanum compound by using the descending symmetry procedure.

Crystal Field Calculations for $La_2MoO_6:Eu^{3+}$

The Eu^{3+} constitutes a very convenient structural probe. Moreover, the crystal field (C.F.) calculations are relatively simpler compared to other ions. It is due to the peculiar situation of the $4f^6$ configuration. Effectively, the ground ^7F septet is well isolated from the rest of the configuration (the energy gap between $^7F_6$ and $^5D_0$ is ~12,000 cm^{-1}). So, the ^7F_J free ion wavefunctions are almost pure. On the other hand, the C.F. operator does not mix states with different multiplicities. As a consequence, it is possible to calculate accurately the C.F. effect by considering only the strongly reduced $^7F_{JM}$ basis, i.e., 49 $|SLJM_J\rangle$ states.

In the absence of polarized emission measurements on single crystals, it is theoretically difficult to perform C.F. calculations on the low C_{2v} symmetry by utilizing only the experimental energy level scheme. Due to the nine nonzero C.F. parameters

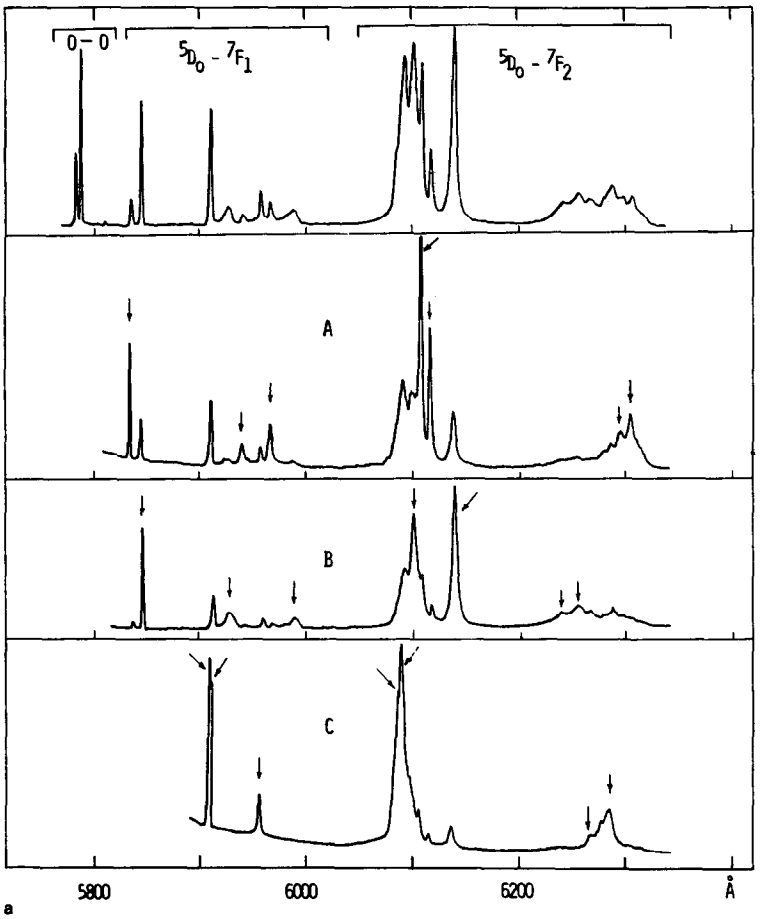

FIG. 3. Part of the fluorescence of $Gd_2MoO_6:Eu^{3+}$ at 77 K. Spectrum A: under laser excitation = 5782 Å; spectrum B: under laser excitation = 5786.5 Å; spectrum C: under laser excitation = 5810 Å. The top spectrum is recorded under uv excitation. Arrows indicate lines corresponding to the excited Eu^{3+} site. (a) The wavelength range 5800–6300 Å. (b) The wavelength range 6900–7100 Å.

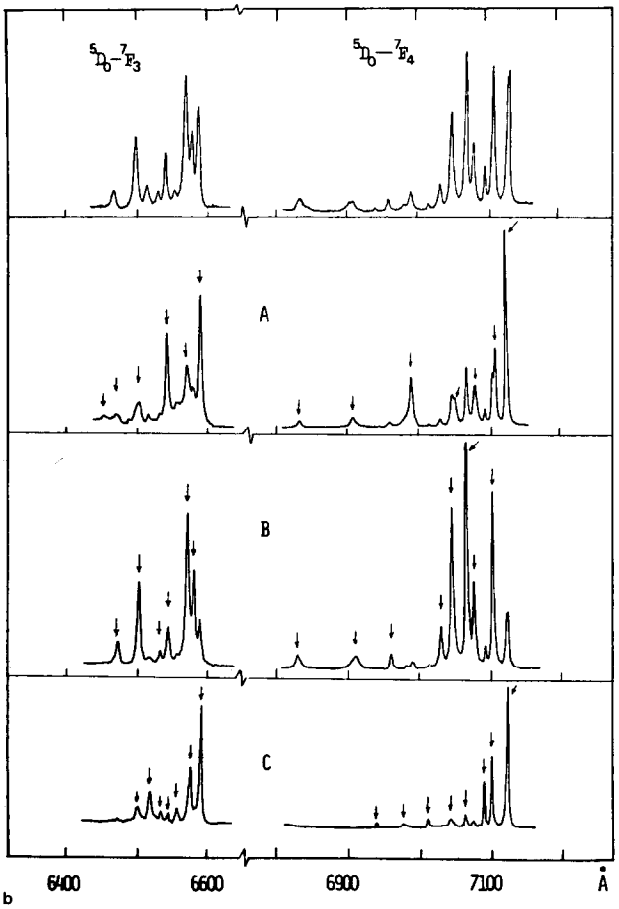

FIG. 3—*Continued.*

allowed by this symmetry it is probably possible to determine several sets of C.F. parameters simulating, more or less correctly, the spectrum. Moreover, from the point charge electrostatic *ab initio* model, it is not realistic to determine starting values of the parameters when complex anions like the MoO_4^{2-} group exist. However, for the specific case of the oxymolybdate we can use the descending symmetry procedure (*22*). For this, we consider that the real point site symmetry—C_2 treated as C_{2v} in our case—is not far from a higher symmetry. Because of the presence of the $(LnO)_n^{n+}$ complex cation as the framework of the structure, the C_{4v} point site is naturally considered as the highest symmetry. The procedure used here is to determine from the energy level scheme the five C.F. parame-

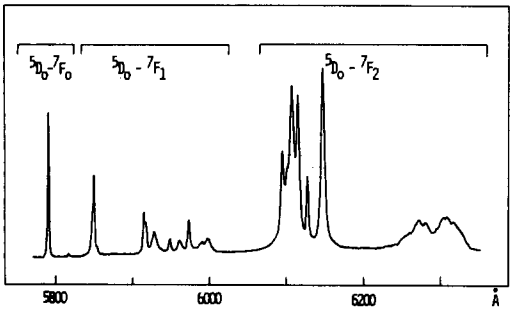

FIG. 4. The characteristic fluorescence spectrum of Y_2MoO_6:Eu^{3+} at 77K under uv excitation.

TABLE II

ENERGY LEVEL SCHEME CONSTRUCTED FROM SELECTIVE EXCITATION OF THE DIFFERENT SITES FOR Gd_2MoO_6: Eu^{3+} AND Y_2MoO_6: Eu^{3+} (ALL UNITS IN cm^{-1})

	Gd_2MoO_6:Eu^{3+}			Y_2MoO_6:Eu^{3+}		
Levels	Site A	Site B	Site C	Site A	Site B	Site C
$^7F_1$	157	173	294	164	172	293
	470	416	297	456	397	300
	543	590	435	525	592	423
$^7F_2$	934	900	790	912	890	792
	962	1003	806	944	998	808
	1432	1276	1271	1413	1319	1282
	1455	1314	1324	1433	1337	1330
$^7F_3$	1803	1830	1826	1793	1827	1833
	1839	1900	1863	1824	1901	1865
	1909	1968	1900	1899	1967	1904
	2007	1993	1923	1984	1993	1920
	2069	2054	1949	2055	2056	1955
	2112	2075	1992	2098	2067	1999
			2023			2028
$^7F_4$	2667	2657	2810	2642	2646	2818
	2823	2819	2890	2806	2824	2900
	2992	2918	2956	2915	2919	2963
	3107	3056	3018	2994	2995	3029
	3162	3088	3056	3058	3060	3060
	3217	3126	3107	3098	3099	3114
	3247	3146	3127	3157	3129	3132
		3197	3170	3203	3150	3175
				3235	3202	
$^5D_0$	17295	17282	17212	17273	17273	17206

ters allowed by C_{4v}, then add extra parameters, characterizing the lowering of the symmetry.

For the C_{4v} symmetry, the C.F. Hamiltonian is written as

$$H_{C_{4v}} = B_0^2C_0^2 + B_0^4C_0^4 + B_4^4(C_{-4}^4 + C_4^4) + B_0^6C_0^6 + B_4^6(C_{-4}^6 + C_4^6).$$

The C_{2v} Hamiltonian is derived by adding four parameters more:

$$H_{C_{2v}} = H_{C_{4v}} + B_2^2(C_{-2}^2 + C_2^2) + B_2^4(C_{-2}^4 + C_2^4) + B_2^6(C_{-2}^6 + C_2^6) + B_6^6(C_{-6}^6 + C_6^6).$$

For the C.F. calculation, we considered the partial energy level scheme deduced from the experiment. The $^7F_4$ level splitting is observed uncompletely. So, we cannot expect a precise determination of B_q^k parameters, especially those of rank 6. Anyhow, when the C_{4v} symmetry is assumed, we can rapidly determine the order of magnitude of B_0^2 from the $^7F_1$ splitting and the rough values of B_0^4 and B_4^4 from the $^7F_2$ splitting. The refinement is conduced by minimization of the root mean square (rms) deviation.

TABLE III

THE CRYSTAL FIELD PARAMETERS OF La_2MoO_6:Eu^{3+} FROM $C_{4v} \rightarrow C_{2v}$ DESCENDING SYMMETRY

		C_{2v}		
Parameters	C_{4v}	Set 1[a]	Set 2[b]	Set 3[b]
B_0^2	−988 ± 37	−995 ± 18	−955 ± 32	−914 ± 16
B_2^2		133 ± 12	88 ± 22	166 ± 9
B_0^4	−1404 ± 44	−1394 ± 22	−1460 ± 37	−1389 ± 20
B_2^4		131 ± 30	165 ± 42	258 ± 19
B_4^4	±657 ± 46	675 ± 22	−629 ± 43	−556 ± 23
B_0^6	−554 ± 142	−600 ± 68	−550 ± 109	−77 ± 35
B_2^6		19 ± 37	−75 ± 139	−1240 ± 24
B_4^6	±717 ± 61	696 ± 29	−700 ± 49	−888 ± 20
B_6^6		36 ± 19	50 ± 37	311 ± 18
σ	15	7	12	6

[a] Set 1 was derived from the positive B_4^4 and B_4^6 for C_{4v}.

[b] Sets 2 and 3 were derived from the negative B_4^4 and B_4^6 for C_{4v}. All values are in units cm^{-1}.

$\sigma = \left(\frac{\Sigma\sigma_i^2}{N-P}\right)^{1/2}$, where σ_i is the individual error, N the number of experimental levels, and P the number of parameters involved. The refining procedure is conducted rapidly by using as starting values the C.F. parameters previously determined for the rare earth oxychloride series (*21*), yielding a rms deviation of 15 cm^{-1} (Table III). Some differences appear with the oxychloride and oxysulfate cases: the absolute value of B_0^4 determined here is higher and B_0^6 has a reverse sign. For the calculation in the C_{2v} symmetry the second and sixth rank C.F. parameters now vary freely. Naturally, because of the initial uncertainty on the relative sign of the B_4^4 and B_4^6 parameters, three different sets can be determined (Table III). The third can probably be immediately eliminated in spite of the best rms deviation, since some of the second rank parameters have a great absolute value, indicating a strong distortion from the C_{4v} symmetry, which is contrary to the initial hypothesis. Probably the first set is the best, with a rms deviation of 7 cm^{-1}. Table IV shows a comparison of the different calculated levels scheme with the experimental one.

TABLE IV

COMPARISON BETWEEN OBSERVED AND CALCULATED ENERGY LEVELS OF Eu^{3+} IN La_2MoO_6 (ALL UNITS IN cm^{-1})

		C_{4v}		C_{2v}					
	E_{exp}	E_{calc}	Irr. rep.	E_{calc} Set 1	Irr. rep.	E_{calc} Set 2	Irr. rep.	E_{calc} Set 3	Irr. rep.
$^7F_0$	0	0	A_1	0	A_1	0	A_1	0	A_1
$^7F_1$	226	217	A_2	215	A_2	222	A_2	228	A_2
	408	443	E	410	B_2	425	B_2	412	B_2
	468	443		474	B_1	454	B_1	462	B_1
$^7F_2$	924	938	E	927	B_1	928	B_2	927	B_2
	950	938		943	B_2	941	B_1	950	B_1
		999	B_2	986	A_1	1002	A_2	1022	A_2
	1146	1147	A_1	1152	A_1	1147	A_1	1140	A_1
	1268	1268	B_1	1267	A_2	1269	A_1	1271	A_1
$^7F_3$	1812	1812	A_2	1810	A_2	1811	A_2	1815	A_2
	1879	1905	E	1890	B_1	1900	B_2	1886	B_2
	1912	1905		1916	B_2	1908	B_1	1909	B_1
	1959	1961	E	1957	B_1	1940	B_2	1950	B_2
	1979	1961		1971	B_2	1979	B_1	1975	B_1
	2054	2049	B_2	2046	A_1	2048	A_2	2054	A_2
	2075	2081	B_1	2078	A_2	2081	A_1	2081	A_1
$^7F_4$		2620	A_1	2621	A_1	2613	A_1	2580	A_1
		2777	A_2	2776	A_2	2767	A_2	2694	B_1
		2864	E	2856	B_1	2829	B_1	2745	A_2
	2872	2864		2869	B_2	2880	B_2	2873	B_2
	2894	2894	B_1	2895	A_1	2890	A_2	2896	A_2
		2939	B_2	2929	A_2	2923	A_1	2926	A_1
	3008	3010	A_1	3010	A_1	3006	A_1	3005	A_1
	3068	3073	E	3068	B_2	3064	B_2	3066	B_2
	3073	3073		3077	B_1	3080	B_1	3078	B_1

Conclusion

We reported here the spectroscopic properties of the Eu^{+3} ion considered as a local structural probe, doping the rare earth molybdates. The point site symmetries deduced from the fluorescence spectra agree quite well with structural studies in the literature. For the gadolinium and yttrium compounds, the Eu^{+3} ions occupy three different point sites, recognized and analyzed by using the site selection technique. Unfortunately, because of the low symmetry of the different point group on one hand, and of the lack of spectroscopic parentage on the other hand, it is not reasonable to perform crystal field simulation which would involve too high a number of parameters. The lanthanum compound shows a completely different spectrum, which can be interpreted in terms of "spectroscopic identity" of the $(LnO)_n^{n+}$ complex cation, showing a great analogy with the spectra of other oxysalts. Then, in spite of the relatively low symmetry of the point site occupied by the rare earth, it was possible to derive accurately the crystal field parameters from the energy levels scheme by using the descending symmetry procedure.

References

1. J. P. Fournier, J. Fournier, and R. Kohlmuller, *Bull. Soc. Chim. Fr.* **12,** 4277 (1970).
2. F. Alekseev, E. Getman, G. Kosheev, and M. Mokhosoev, *Zh. Neorg. Khim.* **14,** 2954 (1969).
3. L. G. Sillen and K. Lundborg, *Z. Anorg. Allg. Chem.* **252,** 2 (1943).
4. G. Blasse, *J. Inorg. Nucl. Chem.* **28,** 1488 (1966).
5. L. H. Brixner, A. W. Sleight, and M. S. Lois, *J. Solid State Chem.* **5,** 186 (1972).
6. L. H. Brixner, A. W. Sleight, and L. M. Foris, *J. Solid State Chem.* **7,** 418 (1973).
7. L. H. Brixner, *Rev. Chim. Mineral. Fr.* **10,** 47 (1973).
8. E. Getman and V. Mokhosoev, *Izv. Akad. Nauk SSSR Neorg. Mater.* **4,** 1554 (1968).
9. C. Gleitzer, *J. Less-Common Met.* **51,** 215 (1977).
10. H. J. Borchardt and P. E. Bierstedt, *Appl. Phys. Lett.* **8,** 50 (1966).
11. K. Aizu, *J. Phys. Soc. Japan* **27,** 387 (1969).
12. G. Blasse and A. Bril, *J. Chem. Phys.* **45,** 2350 (1966).
13. C. Guttel, E. Antic, and P. Caro, *Phys. Status Solidi B* **81,** 463 (1977).
14. N. N. Lebedeva, A. M. Mamedov, and A. R. Mordukhaev, *Mater. Res. Bull.* **15,** 581 (1980).
15. A. F. Wells, "Structure of Inorganic Chemistry," 3rd ed., Oxford Univ. Press (Clarendon), Oxford (1962).
16. P. Caro, *J. Less-Common Met.* **16,** 367 (1968).
17. J. A. Fahey, "12th Proc. R.E. Res. Conf.," 2, 62 (1976).
18. P. Caro, *C. R. Acad. Sci. Paris C* **262,** 992 (1966).
19. P. V. Klevtsov, L. Yu. Kharchenko, and R. F. Klevtsova, *Sov. Phys. Crystallogr.* **20,** 349 (1975).
20. G. Blass and A. Bril, *Philips Res. Rep.* **21,** 368 (1966).
21. K. A. Kuvshinova, M. L. Meil'man, A. G. Smagin, V. I. Voronkova, and V. K. Yanovskii, *Sov. Phys. Crystallogr.* **24,** 559 (1979).
22. J. Hölsä and P. Porcher, *J. Chem. Phys.* **75,** 2108 (1981).
23. D. R. Svoronos, P. Porcher, J. Hölsä, and M. Leshela, to be published.
24. O. K. Moune-Minn and P. Caro, to be published.
25. P. Porcher and P. Caro, *J. Lumin.* **21,** 207 (1980).
26. O. L. Malta, Thèse de Doctorat d'Etat ès-sciences physiques, Université Pierre et Marie Curie de Paris VI (1981).